Optical spectroscopy of pure and doped $CuGeO_3$

A. Damascelli* and D. van der Marel
Solid State Physics Laboratory, University of Groningen, Nijenborgh 4, 9747 AG Groningen, The Netherlands

G. Dhalenne and A. Revcolevschi
Laboratoire de Chimie des Solides, Université de Paris-sud, Bâtiment 414, F-91405 Orsay, France
(Received 2 June 1999; revised manuscript received 13 December 1999)

We investigated the optical properties of $Cu_{1-\delta}Mg_\delta GeO_3$ ($\delta = 0, 0.01$) and $CuGe_{1-x}B_xO_3$ with B = Si ($x = 0, 0.007, 0.05, 0.1$) and Al ($x = 0, 0.01$) in the frequency range 20–32 000 cm^{-1}. We report temperature-dependent reflectivity and transmission measurements, performed with light polarized along the *b* and *c* axes, and optical conductivity spectra obtained by Kramers-Kronig transformation or direct inversion of the Fresnel formula. Special emphasis is given to the far-infrared phonon spectra. The temperature dependence of the phonon parameters is presented and discussed in relation to the soft mode issue in $CuGeO_3$. For $T < T_{SP}$ we detected zone-boundary modes activated by the spin-Peierls phase transition. Following the temperature dependence of these modes, which shows the second-order character of the phase transition, we were able to study the effect of doping on T_{SP}. The optical activity and the polarization of a singlet-triplet excitation detected at 44 cm^{-1}, across the magnetic gap, confirm the existence of the second (optical) magnetic branch recently suggested on the basis of inelastic neutron scattering data. The anisotropy in the magnetic exchange constants along the *b* axis, necessary for the optical triplet mode to gain a finite intensity, and the strong effect of Si substitution on the phonon spectra are discussed in relation to the space group $P2_12_12_1$ recently proposed for $CuGeO_3$ in the high-temperature uniform phase.

I. INTRODUCTION

In 1993 Hase *et al.*[1] concluded, on the basis of magnetic susceptibility measurements, that $CuGeO_3$ shows a spin-Peierls (SP) phase transition, i.e., a lattice distortion that occurs together with the formation of a spin-singlet ground state and the opening of an energy gap in the magnetic excitation spectrum. This magnetoelastic transition is driven by the magnetic energy gain (i.e., suppression of quantum fluctuations) due to dimerization of the antiferromagnetic (AF) superexchange between the spin 1/2 moments of the Cu^{2+} ions [arranged in weakly coupled one-dimensional (1D) CuO_2 chains[2]], which overcompensates the elastic energy loss resulting from the deformation of the lattice.[3,4] In the SP phase, the Cu^{2+} magnetic moments form singlet dimers along the chains and spin-triplet excitations are gapped.[1]

The SP nature of the phase transition in $CuGeO_3$ was inferred from the isotropic drop in the magnetic susceptibility at the transition temperature $T_{SP} = 14$ K and from the reduction of T_{SP} upon increasing the intensity of an applied magnetic field,[1] as theoretically expected for SP systems.[3–6] This initial claim was later confirmed by an impressive variety of experimental results.[7] The gap in the magnetic excitation spectrum was directly observed with inelastic neutron scattering,[8] and its singlet-triplet nature was established with the same technique under application of a magnetic field: A splitting of the single gap into three distinct excitation branches was detected.[9] The dimerization of the Cu^{2+} ions was observed and the lattice distortion very carefully investigated with both neutron and x-ray scattering.[10–12] Finally, the phase transition from the dimerized to the incommensurate phase, expected in magnetic fields higher than a certain critical value,[5,6] was found with field-dependent magnetization measurements at $H_c \approx 12$ T,[13] and the *H-T* phase diagram was studied in great detail.[14]

The discovery of the SP phase transition in $CuGeO_3$ has renewed the interest in this phenomenon, observed previously in organic materials in the 1970s.[15–17] The availability of large high-quality single crystals of pure and doped $CuGeO_3$ made it possible to investigate this magnetoelastic transition by a broad variety of experimental techniques. In this way, the traditional SP theory based on 1D AF chains with only nearest-neighbor (NN) magnetic couplings and a mean-field treatment of the 3D phonon system[3–5] could be tested in all its expectations. Also optical techniques, such as Raman and infrared (IR) spectroscopy, are very useful in investigating magnetic and/or structural phase transitions as they provide information on the nature of the electronic (magnetic) ground state, lattice distortion, and interplay of electronic (magnetic) and lattice degrees of freedom. The aim of our experimental investigation on $CuGeO_3$ with optical spectroscopy was, of course, to detect all possible signatures of the SP phase transition. However, we were in particular interested in a number of issues that could help us in understanding how far the classical SP picture[3,4] is appropriate for the case of $CuGeO_3$:

(i) Analysis of the phonon spectra in order to study the lattice distortion and verify the proposed crystal structures for both the high- and the low-temperature phase.

(ii) Verify the presence of a soft mode in the phonon spectra, upon passing through the SP transition. In fact, a well-defined soft mode is expected in those theoretical models, describing a SP system in terms of a linear coupling between lattice and magnetic degrees of freedom.[5,4]

(iii) Detect possible magnetic bound states and/or a mag-

 ©2000 The American Physical Society

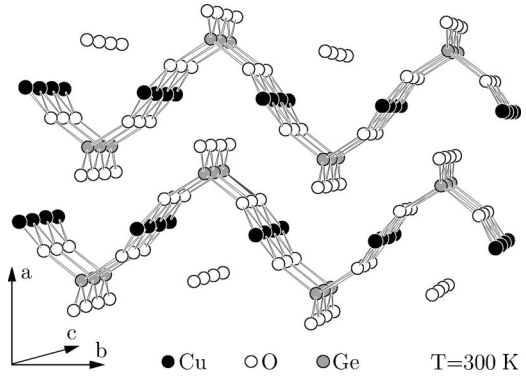

FIG. 1. Crystal structure of $CuGeO_3$ in the high temperature ($T=300$ K) undistorted phase.

netic continuum in the excitation spectrum that could tell us about the symmetry and the order (NNN versus NN) of the magnetic interactions.

(iv) Study the influence of doping on the vibrational and electronic properties and, eventually, on T_{SP}.

Before proceeding to the experimental results, in the next section we will present the group-theoretical analysis[18] of the lattice vibration of $CuGeO_3$ for both the proposed high-temperature undistorted phase[2] and the low-temperature SP phase.[11,12] The number and the symmetry of the theoretically expected IR active phonons will be later compared to the experimental data.

II. GROUP-THEORETICAL ANALYSIS

At room-temperature $CuGeO_3$ has an orthorhombic structure with lattice parameters $a=4.81$ Å, $b=8.47$ Å, and $c=2.941$ Å and space group *Pbmm* ($x\|a$, $y\|b$, $z\|c$) or, equivalently, *Pmma* ($x\|b$, $y\|c$, $z\|a$) in standard setting.[2] The building blocks are edge-sharing CuO_6 octahedra and corner-sharing GeO_4 tetrahedra stacked along the c axis, resulting in Cu^{2+} and Ge^{4+} chains parallel to the c axis. These chains are linked together via the O atoms and form layers parallel to the b-c plane weakly coupled along the a axis (Fig. 1). The unit cell contains two formula units of $CuGeO_3$ (Fig. 2), with site group C_{2h}^y for the two Cu atoms, C_{2v}^z for the two Ge and the two O(1) atoms, and C_s^{xz} for the four O(2) atoms [where O(2) denotes the O atoms linking the chains together].[11,12] Following the nuclear site group analysis method extended to crystals,[19] the contribution of each occupied site to the total irreducible representation of the crystal is

$$\Gamma_{\mathrm{Cu}}=A_u+2B_{1u}+B_{2u}+2B_{3u},$$

$$\Gamma_{\mathrm{Ge+O(1)}}=2[A_g+B_{1u}+B_{2g}+B_{2u}+B_{3g}+B_{3u}],$$

$$\Gamma_{\mathrm{O(2)}}=2A_g+A_u+B_{1g}+2B_{1u}+2B_{2g}+B_{2u}+B_{3g}+2B_{3u}.$$

Subtracting the silent modes ($2A_u$) and the acoustic modes ($B_{1u}+B_{2u}+B_{3u}$), the irreducible representation of the optical vibrations in standard setting (*Pmma*) is

$$\Gamma=4A_g(aa,bb,cc)+B_{1g}(bc)+4B_{2g}(ab)+3B_{3g}(ac)+5B_{1u}(E\|a)+3B_{2u}(E\|c)+5B_{3u}(E\|b). \quad (1)$$

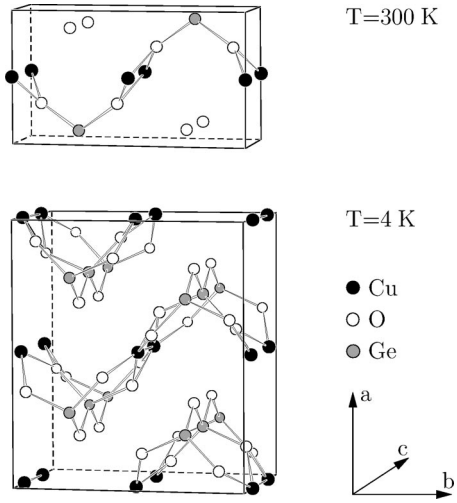

FIG. 2. Conventional unit cell of $CuGeO_3$ in the undistorted (top), and SP phase (bottom). The ion displacements due to the SP transition have been enlarged by a factor of 30.

This corresponds to an expectation of 12 Raman active modes ($4A_g+B_{1g}+4B_{2g}+3B_{3g}$) and 13 IR active modes ($5B_{1u}+3B_{2u}+5B_{3u}$) for $CuGeO_3$, in agreement with the calculation done by Popović *et al.*[20]

At temperatures lower than T_{SP} the proposed crystal structure is still orthorhombic, but with lattice parameters $a'=2a$, $b'=b$, and $c'=2c$ and space group *Bbcm* ($x\|a$, $y\|b$, $z\|c$) or, equivalently, *Cmca* ($x\|c$, $y\|a$, $z\|b$) in the standard setting.[11,12] The distortion of the lattice taking place at the phase transition (Fig. 2) is characterized by the dimerization of Cu-Cu pairs along the c axis (dimerization out of phase in neighboring chains), together with a rotation of the GeO_4 tetrahedra around the axis defined by the O(1) sites (rotation opposite in the sense for neighboring tetrahedra). Moreover, the O(2) sites of the undistorted structure split in an equal number of O(2a) and O(2b) sites, distinguished by the distances O(2a)-O(2a) and O(2b)-O(2b) shorter and larger than O(2)-O(2),[12] respectively. The SP transition is also characterized (Fig. 2) by a doubling of the unit cell (corresponding to a doubling of the degrees of freedom from 30 to 60). The site groups in the new unit cell are C_2^x for Cu, C_2^y for O(1), and C_s^{yz} for Ge, O(2a), and O(2b).[12] Repeating the group-theoretical analysis, we obtain for the contributions to the total irreducible representation:

$$\Gamma_{\mathrm{Cu}}=A_g+A_u+2B_{1g}+2B_{1u}+2B_{2g}+2B_{2u}+B_{3g}+B_{3u},$$

$$\Gamma_{\mathrm{O(1)}}=A_g+A_u+2B_{1g}+2B_{1u}+B_{2g}+B_{2u}+2B_{3g}+2B_{3u},$$

$$\Gamma_{\mathrm{Ge+O(2a)+O(2b)}}=3[2A_g+A_u+B_{1g}+2B_{1u}+B_{2g}+2B_{2u}+2B_{3g}+B_{3u}].$$

Once the silent and the acoustic modes are subtracted, the irreducible representation of the optical vibrations of $CuGeO_3$ in the SP phase (in standard setting *Cmca*) is

$$\Gamma_{\mathrm{SP}}=8A_g(aa,bb,cc)+7B_{1g}(ac)+6B_{2g}(bc)+9B_{3g}(ab)+9B_{1u}(E\|b)+8B_{2u}(E\|a)+5B_{3u}(E\|c). \quad (2)$$

Therefore 30 Raman active modes ($8A_g+7B_{1g}+6B_{2g}+9B_{3g}$) and 22 IR active modes ($9B_{1u}+8B_{2u}+5B_{3u}$) are expected for $CuGeO_3$ in the SP phase, all the additional vibrations being zone-boundary modes activated by the folding of the Brillouin zone.

In order to compare the results obtained for the undistorted and the SP phase of $CuGeO_3$, it is better to rewrite the irreducible representations Γ and Γ_{SP} into *Pbmm* and *Bbcm* settings, respectively, because both groups are characterized by $x\|a$, $y\|b$, and $z\|c$. This can be done by permuting the $(1g,2g,3g)$ and $(1u,2u,3u)$ indices in such a way that it corresponds to the permutations of the axis relating *Pmma* to *Pbmm*, and *Cmca* to *Bbcm*. Therefore, the irreducible representations of the optical vibrations of $CuGeO_3$, for $T>T_{SP}$ (*Pbmm*) and $T<T_{SP}$ (*Bbcm*), respectively, are

$$\Gamma' = 4A_g(aa,bb,cc)+4B_{1g}(ab)+3B_{2g}(ac)+B_{3g}(bc) + 3B_{1u}(E\|c)+5B_{2u}(E\|b)+5B_{3u}(E\|a), \quad (3)$$

$$\Gamma'_{SP} = 8A_g(aa,bb,cc)+9B_{1g}(ab)+7B_{2g}(ac)+6B_{3g}(bc) + 5B_{1u}(E\|c)+9B_{2u}(E\|b)+8B_{3u}(E\|a). \quad (4)$$

It is now evident that the number of IR active phonons is expected to increase from 5 to 8, 5 to 9, and 3 to 5 for light polarized along the *a*, *b*, and *c* axes, respectively.

III. EXPERIMENT

We studied the optical properties of $Cu_{1-\delta}Mg_\delta GeO_3$ (with $\delta=0, 0.01$) and $CuGe_{1-x}B_xO_3$ with $B=$Si ($x=0, 0.007, 0.05, 0.1$) and Al ($x=0, 0.01$) in the frequency range 20–32 000 cm^{-1}. These high-quality single crystals, several centimeters long in the *a* direction, were grown from the melt by a floating zone technique.[21] Platelike samples were easily cleaved perpendicularly to the *a* axis. Typical dimensions were about 2 and 6 mm parallel to the *b* and *c* axis, respectively. The thickness was chosen depending on the experiment to be performed. In reflectivity measurements, when enough material was available, samples several millimeters thick were used in order to avoid interference fringes in the spectra due to Fabry-Perot resonances.[22] Particular attention had to be paid when measuring reflectivity in frequency regions characterized by weak excitations (i.e., from 1000 to 25 000 cm^{-1}): Because of the multiple reflections within the sample these excitations, which would not be directly detectable in reflectivity, would be observable as an absorption with respect to the background dominated by the interference fringes. If a Kramers-Kronig (KK) transformation is performed on such pathological data in order to obtain the optical conductivity, unphysical results would be produced. As a matter of fact, it is precisely for this reason that a charge-transfer excitation at 1.25 eV (10 000 cm^{-1}) was erroneously reported in an early optical paper on $CuGeO_3$.[23] On the other hand, in transmission measurements, where interference fringes cannot be avoided, the thickness of the sample was adjusted to the strength of the particular excitation under investigation.

The samples were aligned by conventional Laue diffraction and mounted in a liquid-He flow cryostat to vary the temperature between 4 and 300 K. Reflectivity and transmission measurements in the frequency range 20–7000 cm^{-1} were performed with a Fourier transform spectrometer (Bruker IFS 113v), with polarized light, in order to probe the optical response of the crystals along the *b* and the *c* axes. In reflectivity a near-normal incidence configuration ($\theta=11°$) was used. Absolute reflectivity and transmission values were obtained by calibrating the data acquired on the samples against a gold mirror and an empty sample holder, respectively. For frequencies higher than 6000 cm^{-1} a Woollam ellipsometer was used in both transmission and reflection operational modes at room temperature. The optical conductivity spectra were obtained by KK transformations in the regions where only reflectivity spectra were measurable, and by direct inversion of the Fresnel equations wherever both reflection and transmission data were available.[22]

IV. PURE $CuGeO_3$

Let us now, as an introduction to what we will discuss in detail in the following sections, describe briefly the main features of the optical spectra of pure $CuGeO_3$ over the entire frequency range we covered with our experimental systems. In Fig. 3 we present room-temperature reflectivity, transmission, and conductivity of $CuGeO_3$ in the frequency range going from 30 to 34 000 cm^{-1}, for $E\|b$ and $E\|c$ (i.e., $\perp$ and $\|$ to the chain direction, respectively). The results are typical of an ionic insulator: The far-infrared (FIR) region ($\omega<1000$ cm^{-1}) is characterized by strong optical phonons, showing the expected anisotropy for the *b* and *c* axes [Fig. 3(a) and 3(c)]; no background conductivity is observable [Fig. 3(c)]. Transmission spectra for $\omega<400$ cm^{-1} are not shown. However, IR transmission measurements carried out at low temperature, in order to investigate very weak magnetic and lattice excitations, will be discussed later in the course of the paper. At frequencies larger than 1000 cm^{-1}, reflectivity is low and almost completely featureless. More information can be gained from transmission in this case. In Fig. 3(b) we can see (in addition to the strong phonons for $\omega<1000$ cm^{-1}) absorption processes at 1330 and 1580 cm^{-1} along the *c* and *b* axes, respectively, and at $\sim$14 000 and $\sim$27 000 cm^{-1}, with approximately the same frequency for the two different axes. Having both reflectivity and transmission data in this region, we could calculate the dynamical conductivity by direct inversion of the Fresnel formula.[22] As shown by Fig. 3(c) and, in particular, by the enlarged view given in the inset (note the very low absolute value of conductivity), extremely weak excitations are present, in the region going from 1000 to 30 000 cm^{-1}, on top of a zero background. Let us now briefly discuss the nature of these excitations. At 1000 cm^{-1} we can see the vanishing tail of the highest *b*-axis phonon [inset of Fig. 3(c)]. Above that, we find the two peaks at 1330 and 1580 cm^{-1} along the *c* and *b* axes, respectively. On the basis of the energy position and of the temperature dependence, these features can be ascribed to multiphonon processes. At $\sim$14 000 cm^{-1} ($\sim$1.8 eV), for both orientations of the electric field, a very weak peak is present, which has been shown to be due to phonon-assisted Cu *d-d* transitions.[24] Finally, the onset of the Cu-O charge-transfer excitations is observable at $\sim$27 000 cm^{-1}. Superimposed to it are some sharper features of probable excitonic nature.

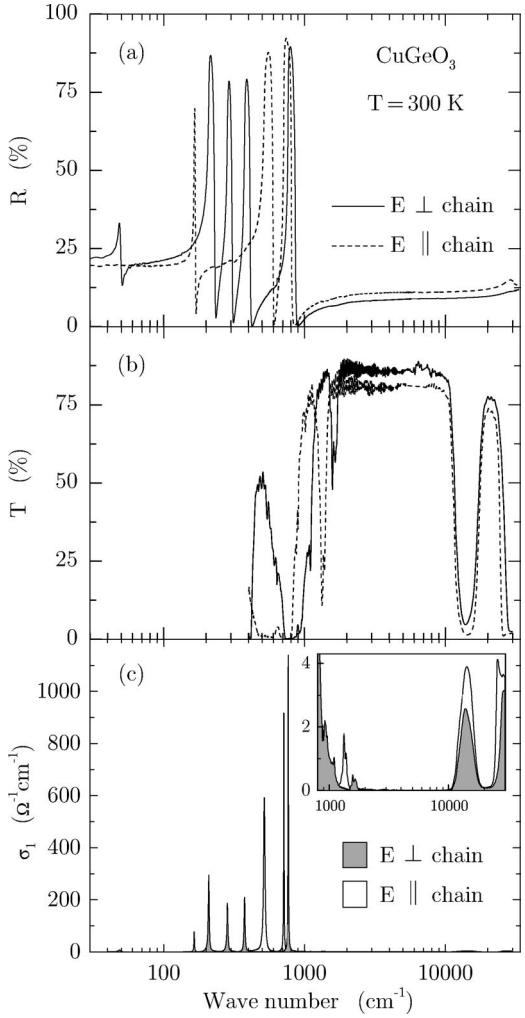

FIG. 3. Room temperature (a) reflectivity, (b) transmission, and (c) optical conductivity of $CuGeO_3$ in the frequency range 30–34 000 cm^{-1} for $E\|b$ and $E\|c$ (i.e., $\perp$ and $\|$ to the chain direction, respectively). Inset: Enlarged view of $\sigma_1(\omega)$ from 800 to 30 000 cm^{-1} (note the very low absolute value).

A. Phonon spectrum and lattice distortion

In this section we will discuss the phonon spectrum of pure $CuGeO_3$, paying particular attention to the zone-boundary folded modes activated by the SP lattice distortion. As the *c*- and *b*-axis (i.e., $E\|$ chain and $E\perp$ chain, respectively, in Fig. 4) reflectivity data have already been discussed in detail in Ref. 25, here we will summarize the main conclusions and move on to the discussion of conductivity and transmission spectra.

In the high-temperature undistorted phase three phonons have been detected along the *c* axis ($\omega_{TO}\approx 167$, 528, and 715 cm^{-1}, for $T=15$ K), and five along the *b* axis ($\omega_{TO}\approx 48$, 210, 286, 376, and 766 cm^{-1}, for $T=15$ K). This is in agreement with what is expected on the basis of the group-theoretical analysis presented in Sec. II [Eq. (3)] for the space group *Pbmm* proposed for $CuGeO_3$ in the uniform phase.[2] The structure in Fig. 4(a) between 200 and 400 cm^{-1} is due to a leakage of the polarizer and corresponds to the three modes detected along the *b* axis in the same frequency range. Similarly, the feature at approximately 630 cm^{-1} in Fig. 4(b) is a leakage of a mode polarized along the *a* axis.[20]

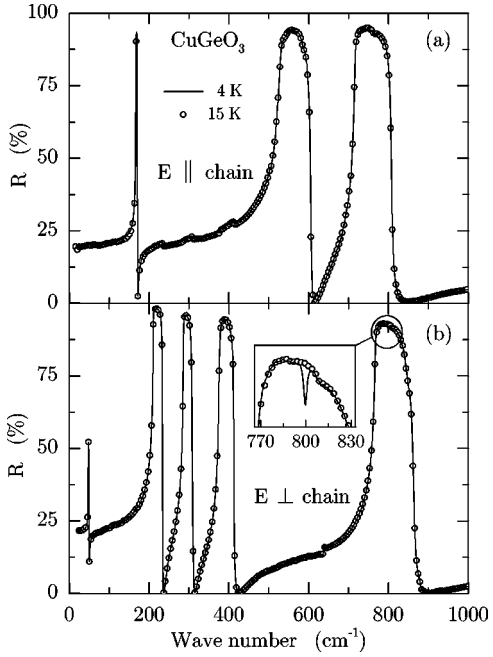

FIG. 4. Reflectivity spectra of pure $CuGeO_3$ in the SP phase (4 K), and just before the SP transition (15 K). The 15 K curves have been plotted with lower resolution, for the sake of clarity. For (a) $E\|$ chain no difference is found across the phase transition whereas for (b) $E\perp$ chain a new feature appears at 800 cm^{-1} (as clearly shown in the inset).

However, the reason why this phonon has been detected in the *b*-axis reflectivity is not simply, as in the previous case, a leakage of the polarizer. It has to do with the finite angle of incidence $\theta=11°$ of the radiation on the sample, and with the fact that *p*-polarized light was used to probe the optical response along the *b* axis. In fact, whereas for *s*-polarized light the electric field was parallel to the *b*-*c* plane, in *p* polarization there was a small but finite component of the electric vector perpendicular to the plane of the sample, which could then couple to the *a*-axis excitations (at least to those particularly intense).

In the low-temperature phase only one new feature was directly observable in reflectivity: A dip at 800 cm^{-1} for $E\|b$ (inset of Fig. 4).[25] A careful investigation of temperatures ranging from 4 to 15 K (Fig. 10) indicated that this feature, which falls in the frequency region of high reflectivity for the B_{2u}-symmetry mode at 766 cm^{-1} and therefore shows up mainly for its absorption, is a zone-boundary folded mode activated by the SP transition.[25]

Whereas the number of IR active phonons is expected to increase from 5 to 8, 5 to 9, and 3 to 5 for light polarized along the *a*, *b*, and *c* axes, respectively [see Eqs. (3) and (4)], only one SP activated mode was observed. On the other hand, more lines can be found by means of a deeper analysis, in agreement with the results reported in Ref. 26: By checking the optical conductivity at 4 and 15 K, a second folded mode is present along the *b* axis at 310 cm^{-1} (see Fig. 5). This line was not distinguishable in reflectivity because it coincides with ω_{LO} of the B_{2u}-symmetry phonon at 286 cm^{-1}. It has to be mentioned that the remnant peak observable in the 15 K data at 313 cm^{-1} is an experimental glitch;

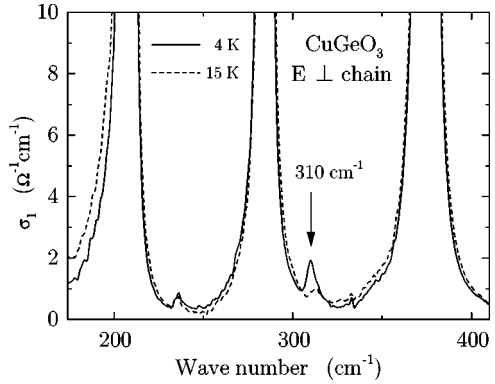

FIG. 5. Conductivity spectra of pure $CuGeO_3$ in the SP phase (4 K), and just before the SP transition (15 K), for $E\perp$ chain: A SP activated mode is observable at 310 cm^{-1}.

it does not have any temperature dependence (it is there also at 300 K) and, therefore, it is not related to the phase transition.

In order to probe the phonon spectrum of the dimerized phase with a more sensitive tool, we performed transmission measurements on a 350 μm thick sample in the FIR region. One additional line was then detected at 284 cm^{-1} along the *c* axis, as shown in Fig. 6. In the top panel a transmission spectrum acquired at 4 K is plotted in the frequency range 100–300 cm^{-1}. Fabry-Perot interference fringes are clearly visible, interrupted at $\sim$167 cm^{-1} by the strong absorption of the lowest-energy B_{1u}-symmetry phonon. At 284 cm^{-1} one can observe a slightly more pronounced minimum in the interference pattern. Because of the weakness of this line, a real peak can be observed only in the absorbance difference spectrum (bottom panel of Fig. 6). The spikes present at $\sim$167 cm^{-1} in the absorbance difference spectrum are due to the complete absorption of the light in that frequency range (top panel). As a last remark, we want to stress that the final assignment of the 310 and 284 cm^{-1} peaks to optical phonons activated by the SP transition is based, as for the line at 800 cm^{-1}, on their temperature dependence (not shown).

B. Phonon parameters and the soft-mode issue

As far as the dynamical interplay between spins and phonons in $CuGeO_3$ is concerned, it is clear from the reflectivity spectra plotted in Fig. 4 that a well-defined soft mode, driving the structural deformation in $CuGeO_3$, has not been detected in our measurements. However, as any dimerization must be related to normal modes away from the zone center, the softening of one or more modes across the SP phase transition should be expected at $k=(\pi/a,0,\pi/c)$, the actual propagation vector in $CuGeO_3$. As optical techniques can probe the phonon branches only at the Γ point ($k=0$), the softening can, strictly speaking, be investigated only by neutron scattering. Nevertheless, we tried to gain interesting insights from the temperature dependence of the phonon parameters obtained from the fit of the reflectivity data (see Fig. 7 and Table I). In fact, if the dispersion and the mixing of the phonon branches are not too strong, the presence of a soft mode at $k=(\pi/a,0,\pi/c)$ could result in an overall softening of the branch it belongs to. Our first attempt was to check if any of the IR phonons was showing a red shift upon cooling the sample. In Fig. 7 we can see that the B_{2u} mode ($E\perp$ chain) at 48 cm^{-1} is the only one showing an evident monotonic red shift from 300 to 15 K. Below T_{SP} this mode shows only a small blue shift. Also the behavior of its oscillator strength is rather interesting: It grows continuously from 300 to 15 K (a $\sim$23% increase), and it suddenly drops $\sim$15% across the phase transition. On the basis of this results, we concluded that these particular phonon branch

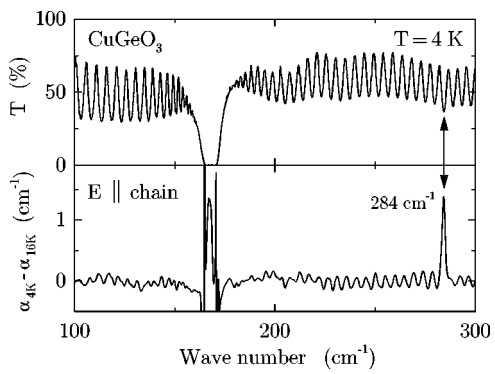

FIG. 6. Transmission of pure $CuGeO_3$ in the SP phase for $E\|$ chain (top). In the absorbance difference spectrum a SP activated mode is observable at 284 cm^{-1} (bottom).

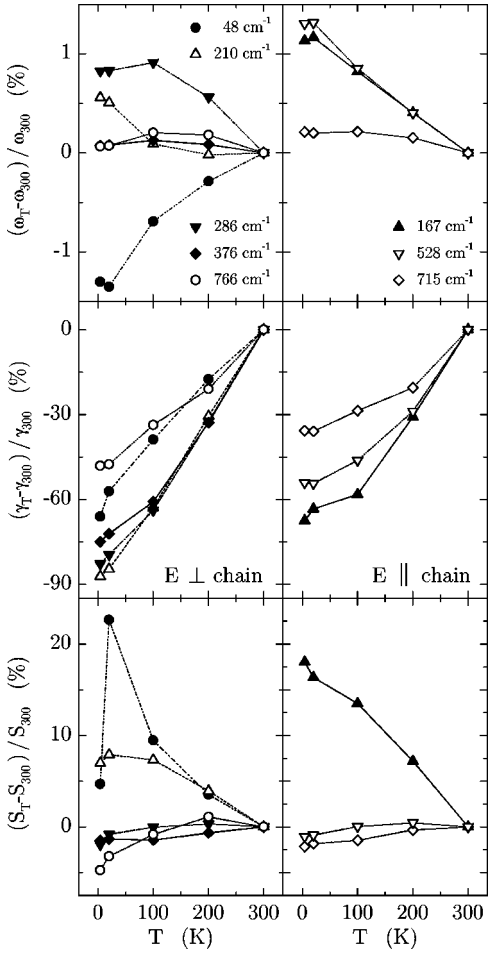

FIG. 7. Temperature dependence of percentage change in resonant frequency, damping, and oscillator strength (from top to bottom) of the IR phonons of pure $CuGeO_3$ in the undistorted phase, for $E\perp$ chain (left) and $E\|$ chain (right).

TABLE I. Resonant frequency ω_{TO} (cm^{-1}), damping γ (cm^{-1}), and oscillator strength S of the IR phonons detected for $E\|$ chain (B_{1u} symmetry) and $E\perp$ chain (B_{2u} symmetry) on pure $CuGeO_3$. The parameters have been obtained by fitting the phonon spectra with Lorentz oscillators.

Mode	Param.	4 K	15 K	100 K	200 K	300 K
	ω_{TO}	166.78	166.82	166.25	165.56	164.90
B_{1u}	γ	0.41	0.46	0.53	0.88	1.27
	S	0.348	0.343	0.335	0.316	0.295
	ω_{TO}	527.69	527.74	525.33	522.98	520.89
B_{1u}	γ	4.07	4.05	4.78	6.32	8.89
	S	1.900	1.903	1.921	1.929	1.921
	ω_{TO}	715.25	715.17	715.27	714.84	713.75
B_{1u}	γ	3.12	3.11	3.46	3.85	4.85
	S	0.636	0.638	0.640	0.648	0.650
	ω_{TO}	48.28	48.26	48.58	48.78	48.92
B_{2u}	γ	0.63	0.79	1.13	1.52	1.85
	S	0.286	0.335	0.299	0.282	0.273
	ω_{TO}	210.27	210.17	209.29	209.07	209.10
B_{2u}	γ	0.44	0.53	1.28	2.41	3.46
	S	1.717	1.732	1.723	1.669	1.605
	ω_{TO}	285.79	285.79	286.03	285.04	283.45
B_{2u}	γ	0.83	0.99	1.75	3.27	4.84
	S	0.765	0.773	0.780	0.782	0.780
	ω_{TO}	375.62	375.65	375.81	375.66	375.35
B_{2u}	γ	1.44	1.60	2.26	3.86	5.76
	S	0.596	0.597	0.596	0.601	0.605
	ω_{TO}	766.28	766.34	767.35	767.16	765.79
B_{2u}	γ	3.27	3.30	4.18	4.98	6.30
	S	0.677	0.689	0.705	0.718	0.711
	ω_{TO}	284.21	-	-	-	-
$B_{1u,SP}$	γ	—	-	-	-	-
	S	—	-	-	-	-
	ω_{TO}	309.58	-	-	-	-
$B_{2u,SP}$	γ	4.27	-	-	-	-
	S	0.003	-	-	-	-
	ω_{TO}	799.75	-	-	-	-
$B_{2u,SP}$	γ	2.32	-	-	-	-
	S	0.0007	-	-	-	-

could have been a good candidate to show a real softening at the SP distortion vector in the Brillouin zone.

In order to check this hypothesis more directly, we performed transmission measurements with a millimenter-wave transmission setup, equipped with a backward wave oscillator operating in the frequency range 3.6–6.0 cm^{-1}.[27] The measurements were done on a ~ 1 mm thick sample of pure $CuGeO_3$ and, in order to relax the k-conservation rule and to obtain a result averaged over the entire Brillouin zone, on Si and Mg substituted crystals with approximately the same thickness of the pure $CuGeO_3$. In this way, we aimed to measure very accurately the transmission through the samples at one very low fixed frequency (5 cm^{-1}) as a function of temperature. If a mode would get soft, it would possibly result in a temperature-dependent transmission showing a w shape centered at T_{SP}: two minima in the absolute transmission, one on each side of T_{SP}. Unfortunately, we could not detect any change. Had we seen the expected w-shape behavior, this would have been a strong indication of the existence of a soft mode in $CuGeO_3$. In the present case we cannot confirm nor rule out a soft mode.

Recently, it was shown using neutron scattering that the preexisting soft mode, expected in the classical theories of the SP phase transition,[5,4] is not there in the case of $CuGeO_3$.[28] Neither present is the central peak usually observed in order-disorder phase transitions.[29] As a consequence of these findings, it appears that the behavior of the phonon parameters for the B_{2u} mode at 48 cm^{-1} is simply ''accidental.'' One may speculate that the absence of a softening at $k=(\pi/a,0,\pi/c)$ implies that the phase transition is not driven by a softening of the phonon spectrum at $k=(\pi/a,0,\pi/c)$, but only by a change in electronic structure, which, in turn, determines the dynamical charge of the ions and the interatomic force constants. In this scenario, the large change in oscillator strength of some of the vibrational modes observed in our optical data (Fig. 7), results from a change in ionicity, or, in other words, a transfer of spectral weight from the elastic degrees of freedom to electronic excitations.

V. DOPED $CuGeO_3$

In this section we will present the optical spectra of $Cu_{1-\delta}Mg_\delta GeO_3$ (with $\delta = 0, 0.01$) and $CuGe_{1-x}B_xO_3$ [with $B=$ Si ($x=0, 0.007, 0.05, 0.1$) and Al ($x=0, 0.01$)] single crystals. We investigated, as we did for the pure material, the phonon spectrum as a function of temperature of Mg- and Si-substituted $CuGeO_3$, by means of reflectivity measurements in the FIR region (Sec. V A). The aim of this investigation was, first of all, to study the effect of doping on the SP phase transition; second, to verify the recent claims of Yamada and co-workers,[30,31] who suggested that the structure originally proposed for $CuGeO_3$ in the high-temperature undistorted phase[2] could be wrong. In addition, transmission measurements in the mid-infrared (MIR) region were performed on all the samples, in order to detect possible electronic and/or magnetic excitations that could provide us with additional information about the interplay of spin and charge in this quasi-1D system (Sec. V B).

A. Far-infrared reflection

The 4 K reflectivity data acquired on Si doped samples for $E\|$ chain (c axis) and $E\perp$ chain (b axis) are shown in Figs. 8(a) and 8(b), respectively. The spectra are similar to those we already discussed for pure $CuGeO_3$. However, some new features, stronger in intensity the higher the Si concentration, are observable already at room temperature. Therefore, they are due to the substitution of Ge with the lighter Si and not directly related to the SP transition: new phonon peaks at 900 cm^{-1}, along the c axis [Fig. 8(a)], and at 500 and 960 cm^{-1}, along the b axis [Fig. (8(b)]. Moreover, the much more complicated line shape and the considerable reduction of oscillator strength of the high-frequency phonons indicate first, a strong Ge (Si) contribution to these modes, mainly due to O vibrations,[20] and second, that substituting Si for Ge has apparently a strong symmetry-lowering effect, a point

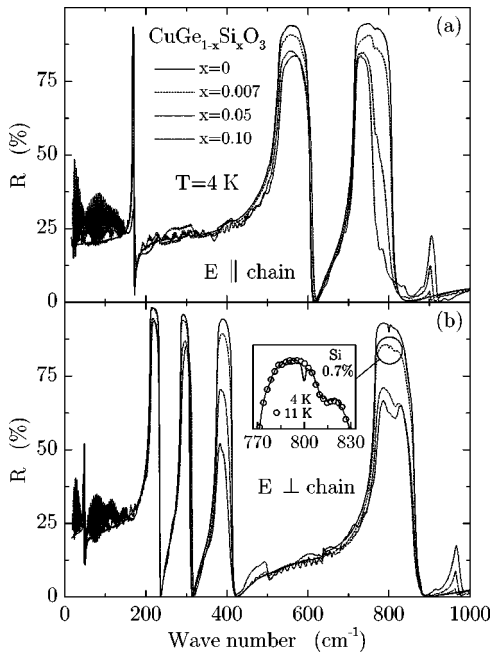

FIG. 8. (a) *c*-axis and (b) *b*-axis reflectivity spectra of Si-doped $CuGeO_3$ at 4 K for different Si concentrations. For 0.7% Si substitution the 800 cm^{-1} *b*-axis folded mode, activated by the SP transition, is clearly observable in the inset of panel (b) where the 4 K and the 11 K data are compared.

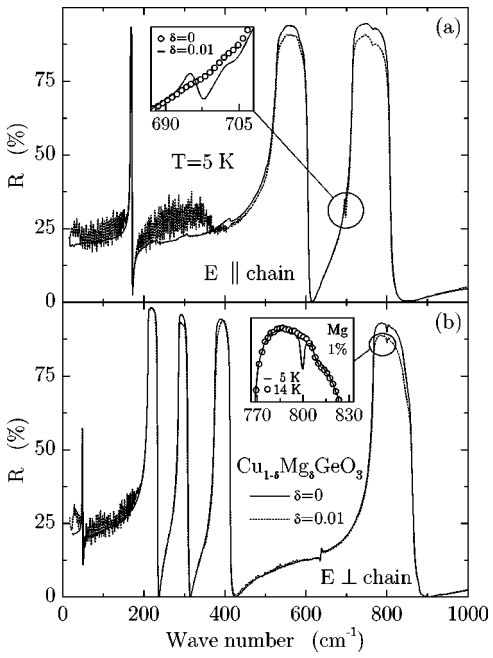

FIG. 9. (a) *c*-axis and (b) *b*-axis reflectivity spectra of pure and 1% Mg-doped $CuGeO_3$, at 5 K. Inset of panel (a): Enlarged view of the frequency region around 700 cm^{-1}. The additional peak observed for Mg doping is due to the mass difference between Cu and Mg and it is not related to the SP transition. The 800 cm^{-1} *b*-axis folded mode, activated by the SP transition, is still observable for 1% Mg-doping by comparing the 5 K and the 14 K data [inset of panel (b)].

that we will discuss again later in relation to the claim of Yamada *et al.*[30,31] about a possible lower symmetry with respect to the one originally proposed by Völlenkle *et al.*[2] for the uniform structure of $CuGeO_3$. The SP-activated zone-boundary mode at 800 cm^{-1} (previously detected on pure $CuGeO_3$ for $E\perp$ chain) is found only for the lowest Si concentration. This is clearly shown in the inset of Fig. 8(b), where the 4 and 11 K data are compared. We can conclude that up to 0.7% Si doping the SP transition is still present with $T_{SP}<11$ K, whereas for 5% and 10% Si concentrations no signature of the transition could be found in reflectivity (nor in conductivity nor in transmission, as a matter of fact).

The 5 K results obtained on the 1% Mg-doped sample are plotted, together with the results obtained on pure $CuGeO_3$, in Figs. 9(a) and 9(b), for $E\|$ chain (*c* axis) and $E\perp$ chain (*b* axis), respectively. Clearly, Mg doping is affecting the optical response of $CuGeO_3$ less than Si doping. A new phonon, due to the mass difference between Cu and Mg, is present in the *c*-axis spectra at 695 cm^{-1}, as shown in the inset of Fig. 9(a). For $E\perp$ chain we observe the 800 cm^{-1} zone-boundary mode activated by the SP transition [see inset of Fig. 9(b)]. For the 1% Mg-doped sample, T_{SP} seems to be lower than that in pure $CuGeO_3$; on the other hand, the structural deformation is not as strongly reduced as in the 0.7% Si-doped sample, as can be deduced from the direct comparison between the insets of Fig. 8(b) and Fig. 9(b).

Performing careful reflectivity measurements for temperatures ranging from 4 to 15 K on pure, 1% Mg, and 0.7% Si-doped samples, we cannot only determine the character of the phase transition, but also estimate more precisely the reduction of the oscillator strength for the 800 cm^{-1} phonon and, eventually, the doping dependence of T_{SP}. For such a quantitative analysis it is easier to fit with Lorentz oscillators not the reflectivity but the optical conductivity data [e.g., see inset of Fig. 10(a), where the fit of the 4 K data is presented]. In fact, in the latter case the SP-activated mode at 800 cm^{-1} appears as an additional peak superimposed on the Lorentzian tail of the 766 cm^{-1} B_{2u} phonon of the high-symmetry phase, and its oscillator strength is directly proportional to the area under the peak. In Fig. 10 we can observe, for the three different samples, the gradual disappearance of the activated phonon for $T\rightarrow T_{SP}$ from below. The oscillator strength plotted versus temperature [inset of Fig. 10(c)] clearly shows, for pure $CuGeO_3$, the second-order character of the phase transition. Like the intensity of the superlattice reflections measured with x-ray or neutron scattering, the intensity of the zone-boundary folded modes in an optical experiment also is proportional to δ^2, where δ denotes the generalized symmetry-breaking lattice distortion (see Ref. 29). Therefore, the temperature dependence of the oscillator strength for the 800 cm^{-1} mode can be fitted to the equation $\sim(1-T/T_{SP})^{2\beta}$. The best fit value of β is strongly dependent on the temperature range chosen to fit the data. If only points very close (within 1 K) to T_{SP} are considered, for pure $CuGeO_3$ the value $\beta=0.36\pm0.03$ is obtained, as reported in Ref. 32. At this point, in relation to the soft-mode issue in $CuGeO_3$, it is worth mentioning that for the organic SP system TTF-$CuS_4C_4(CF_3)_4$, which shows a precursive 3D soft phonon at the superlattice position, the value $\beta=0.5$ was obtained.[33] It was argued by Cross and Fisher[4] that this soft mode is responsible for the mean-field behavior, i.e., $\beta=1/2$, in the TTF salt. For the doped samples, in contrast to the pure system, it is not possible to fit the temperature de-

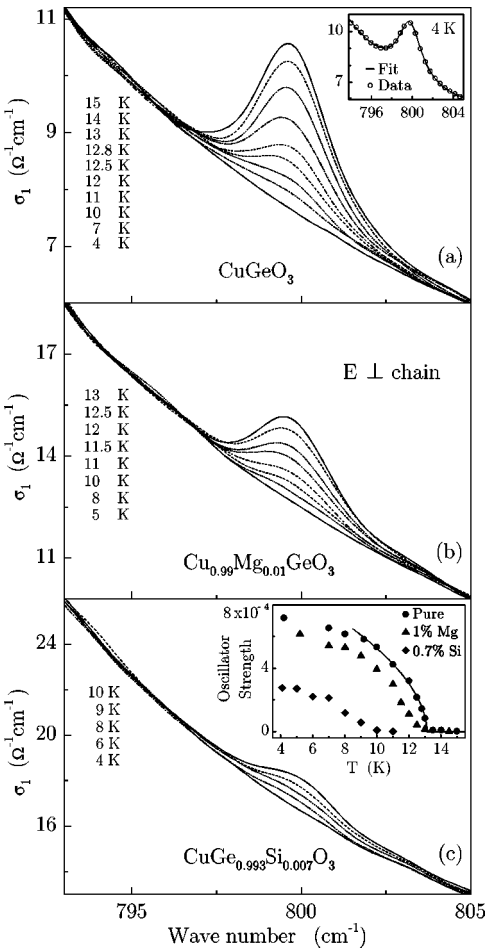

FIG. 10. Enlarged view of the *b*-axis optical conductivity for (a) pure, (b) 1% Mg-, and (c) 0.7% Si-doped $CuGeO_3$: The detailed temperature dependence of the 800 cm^{-1} SP-activated mode is shown. Inset of panel (a): Lorentz fit of the 4 K data (plotted with reduced resolution) for pure $CuGeO_3$. Inset of panel (c): Oscillator strength of the SP mode plotted vs. temperature; for pure $CuGeO_3$ the fit to the equation $(1-T/T_{SP})^{2\beta}$ with $\beta=0.36$ is also shown.

pendence of the oscillator strength to the equation $\sim(1-T/T_{SP})^{2\beta}$. In fact, the oscillator strength versus T curves plotted in the inset of Fig. 10(c) for the doped crystals are characterized by an upturned curvature near T_{SP}. This effect can be explained in terms of a distribution of transition temperatures due to the disorder introduced upon doping the system.[34] However, for the 1% Mg- and the 0.7% Si-substituted samples the estimates for T_{SP} of approximately 12.4 and 9.3 K, respectively, can be obtained. Considering that usually for pure $CuGeO_3$ $T_{SP}\approx 14.2$ (on our pure sample a slightly reduced value has been observed), we can conclude that Si is three times more effective in reducing T_{SP} than Mg. This result has recently been confirmed, on a stronger basis, by a very systematic and detailed investigation of the decrease of T_{SP} and of the occurrence of 3D AF order at lower temperature on several doped single crystals of $CuGeO_3$ by magnetic susceptibility measurements.[35]

The difference between Mg and Si in influencing T_{SP} can be understood considering their different effect on the magnetism of the system. The substitution of a Cu^{2+} ion by a nonmagnetic impurity, like Mg, cuts a CuO_2 chain in two segments by breaking a singlet dimer; a free $S=1/2$ Cu^{2+} spin is created for each Mg impurity. More subtle is the effect of replacing Ge with Si: One could at first glance expect a weak effect because Si is not directly breaking a dimer. On the other hand, Khomskii *et al.* showed that Si weakens the side-group effect,[36,37] which is responsible for the superexchange being AF in $CuGeO_3$ [as the Cu-O(2)-Cu bond angle is $\gamma\approx 98°$, on the basis of the Goodenough-Kanamory-Anderson rule[38] the superexchange should be (weakly) ferromagnetic]. Because Si is smaller than Ge, the Si-O hybridization is smaller than the Ge-O one. As a result, Si breaks the AF Cu-Cu interaction on the two CuO_2 chains adjacent to the Si^{4+} ion.[36,37] This explains, at least qualitatively, why Si has a stronger effect on T_{SP} than Mg. To fully understand why Si is three times and not only twice as efficient as Mg in reducing T_{SP}, we believe that the effect of Si substitution on the NNN (i.e., not only NN) exchange interaction should also be taken into account.

Recently, on the basis of electron paramagnetic resonance experiments, Yamada *et al.* raised doubts about the room-temperature structure of $CuGeO_3$.[30] X-ray diffraction experiments were then performed by Hidaka *et al.* on pure single crystals grown by the floating-zone method and subsequently improved by a combined annealing and slow cooling process.[31] The space group was determined to be $P2_12_12_1$, with a unit cell eight times larger $(2a\times b\times 4c)$ than the one originally proposed by Völlenkle *et al.*[2] The irreducible representation of the optical vibrations for the space group $P2_12_12_1$ is

$$\Gamma''=56A(aa,bb,cc)+55B_1(ab;E\|c)+63B_2(ac;E\|b)+63B_3(bc;E\|a), \quad (5)$$

corresponding to 63, 63, and 55 optical active modes along the *a*, *b*, and *c* axes, respectively. The absence of these modes in our infrared spectra of pure $CuGeO_3$ (see Sec. IV A) suggests that the the superlattice modulation corresponding to the $P2_12_12_1$ space group is too weak to provide a detectable oscillator strength for the extra modes (possibly because the deformation of the structure would be there only on a local scale on noncarefully annealed single crystals).[31] In this context, the results obtained on Si-substituted $CuGeO_3$ might be more significant. In Fig. 11, the low-temperature optical conductivity of pure and 10% Si-doped $CuGeO_3$, for (a) $E\|$ chain and (b) $E\perp$ chain, is plotted. We can observe a reduction of oscillator strength and a broadening for all the lattice vibrations. Moreover, additional bands appear over the entire range, as clearly shown in Fig. 12, where the low-temperature optical conductivity, for all the measured Si-doped samples, is presented. We can see that not only sharp peaks appear at 900 and 960 cm^{-1} along the *c* and *b* axes, respectively, as discussed at the beginning of this section. There is also a large number of phonon bands, growing in intensity upon increasing the Si concentration, at both low and high frequencies. Because the introduction of impurities in a crystal results in a relaxation of the *k*-conservation rule, states with $k\neq 0$ are projected back to the Γ point, and phonon bands averaged over the Brillouin zone can be measured in an optical experiment. This explains qualitatively the complex phonon sideband structure in Figs. 11 and 12. On the other hand, because analogous phonon sidebands are not present for Mg- and Al-substituted

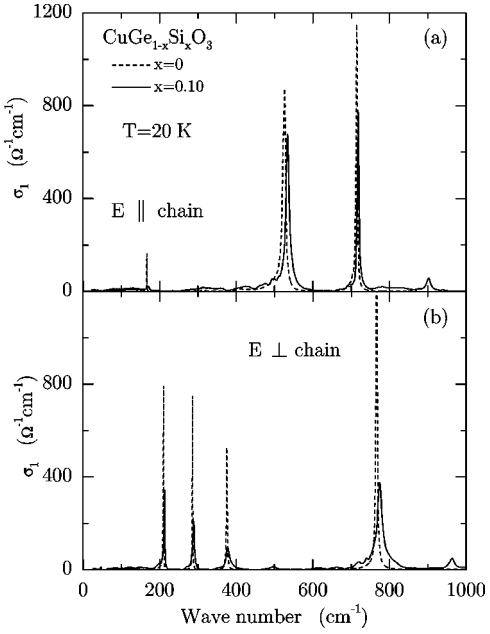

FIG. 11. Optical conductivity at 20 K, obtained by KK analysis, on pure and 10% Si-doped $CuGeO_3$, for (a) $E\|$ chain and (b) $E\perp$ chain. In panel (b) the pure $CuGeO_3$ data have been clipped in order to use the same scale as in panel (a): The peak value of the phonon at 766 cm^{-1} is 2010 $\Omega^{-1}cm^{-1}$.

$CuGeO_3$, we may speculate that Si, which has such a strong influence on T_{SP} via the side-group effect,[36,37] could also be responsible for enhancing the underlying lattice distortion proposed by Yamada and co-workers.[30,31] In our opinion these results, although not conclusive, indicate that a symmetry lower than the one assumed until now could be possible.

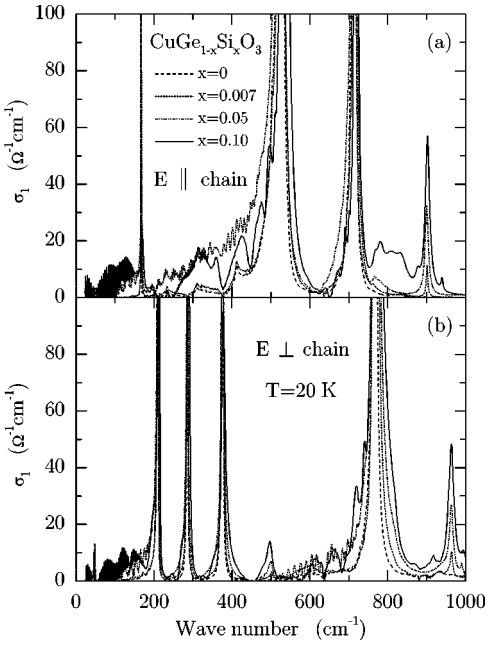

FIG. 12. Optical conductivity at 20 K, obtained by KK analysis, on pure and several Si-doped $CuGeO_3$ crystals (a) for $E\|$ chain and (b) $E\perp$ chain.

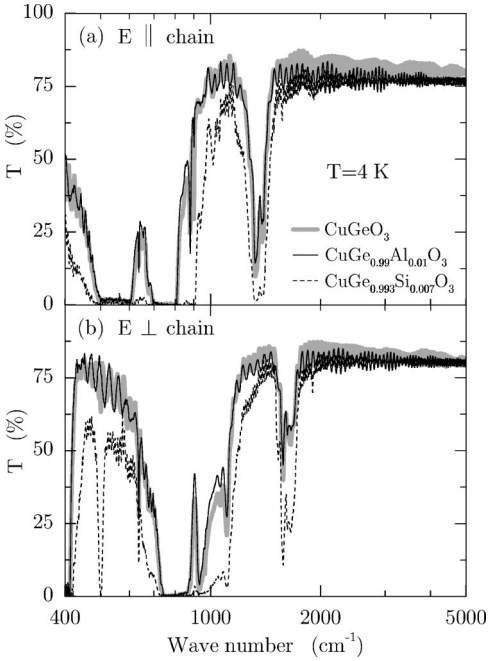

FIG. 13. Transmission spectra (4 K) on pure, 1% Al-, and 0.7% Si-doped $CuGeO_3$ for (a) $E\|$ chain and (b) $E\perp$ chain.

B. Mid-infrared transmission

In this section we will discuss the optical data obtained by performing transmission experiments, in the range 400–8000 cm^{-1}, on $Cu_{1-\delta}Mg_\delta GeO_3$ (with $\delta=0, 0.01$) and $CuGe_{1-x}B_xO_3$ with B=*Si* ($x=0, 0.007, 0.05, 0.1$) and Al ($x=0, 0.01$). From reflectivity and transmission, we calculated the optical conductivity by direct inversion of the Fresnel formula.[22] We aimed to study whether doping has an effect on the electronic and/or magnetic excitations similar to what has been observed on the underdoped parent compounds of high-T_c superconductors.[39,40] On the latter materials, chemical substitution introduces charge carriers in the 2D Cu-O planes, resulting in a disappearance of the gap and in the transfer of spectral weight into a Drude peak for the in-plane optical response. In addition, the so-called MIR band, whose interpretation is still controversial, is usually present in these systems.[39,40]

The 4 K transmission spectra of pure, 1% Al-, and 0.7% Si-doped $CuGeO_3$, for $E\|$ chain and $E\perp$ chain, are plotted in Figs. 13(a) and 13(b), respectively. Spectra at different temperatures above and below the phase transition were measured. However, the results are not shown because no particular temperature dependence was observed. Similarly, the spectra for 1% Mg- and 5 and 10% Si-doped crystals are not presented because no additional information can be obtained. As shown in Fig. 13, the transmission through pure $CuGeO_3$ in this frequency region is mainly characterized by the strong absorptions of the phonons of the high-symmetry phase at 528 and 715 cm^{-1}, along the *c* axis, and at 376 and 766 cm^{-1}, along the *b* axis. In addition, multiphonon bands are present, the most intense ones being at 1330 and 1580 cm^{-1} along the *c* and *b* axes, respectively. The same features are observable on the doped samples where more multiphonon bands are detected reflecting the presence of additional peaks in the single-phonon spectrum (as discussed on the basis of reflectivity data). A last remark has to be made about the

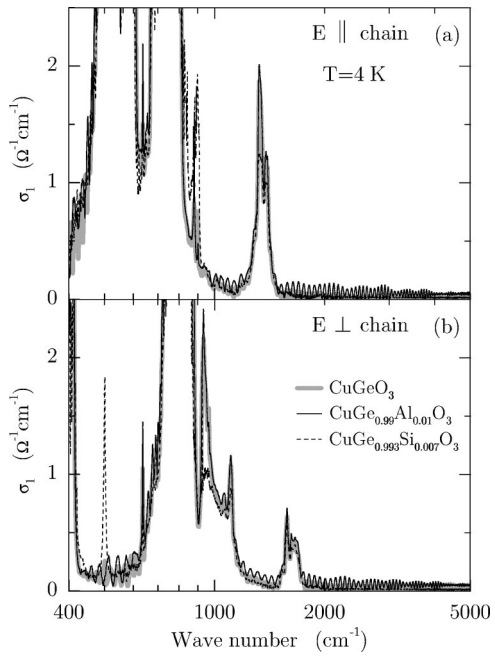

FIG. 14. Conductivity spectra at 4 K, obtained by direct inversion of the Fresnel formula, on pure, 1% Al-, and 0.7% Si-doped $CuGeO_3$, for (a) $E\|$ chain and (b) $E\perp$ chain. Note the very low value of $\sigma_1(\omega)$.

oscillations present in all the spectra of Fig. 13. These are interference fringes due to Fabry-Perot resonances;[22] the different periods of the interference patterns are due to the different thickness of the samples.

If we now consider the optical conductivity spectra plotted in Fig. 14, it is clear that nothing else has been detected, in this frequency range, besides absorption processes purely related to lattice degrees of freedom. In particular, for all the sample, the conductivity is just zero from 2000 to 8000 cm^{-1}. From these results and from the fact that no signature of a Drude peak was observed in any of the doped samples in reflectivity experiment, we conclude that no charge carriers are introduced in $CuGeO_3$ by the different chemical substitutions we tried nor magnetic/dielectric polarons (observed,[40] e.g., in ultra-low-doped $YBa_2Cu_3O_6$). One has to note that, in this sense, the most significant of the results we showed is the one obtained on Al-substituted $CuGeO_3$ because in this case, contrary to Si substitution, Ge is replaced by an element with different valence.

VI. DISCUSSION

In our investigation of pure and doped $CuGeO_3$ with optical spectroscopy we observed features that are not completely understandable on the basis of Cross and Fisher theory for the SP phase transition[4] and of the achieved picture of the SP transition in $CuGeO_3$. No preexisting soft mode was detected, not only in our optical measurements but especially in neutron scattering experiments.[28] This result could explain why the value of β in the expression describing the temperature dependence of the order parameter close to T_{SP} $[\delta\sim(1-T/T_{SP})^{\beta}]$ deviates in $CuGeO_3$ from the mean-field behavior $\beta=1/4$ observed in the TTF salt. Finally, large changes in the phonon spectrum were observed for Si substitution, which might be in favor of the alternative space group $P2_12_12_1$ recently proposed for $CuGeO_3$ in the high-temperature uniform phase.[30,31]

Many attempts have recently been made to improve the understanding of the SP phase transition in $CuGeO_3$. In particular, it has been shown that the adiabatic treatment of the 3D phonon system, characteristic for the Cross and Fisher theory,[4] is not appropriate for the case of $CuGeO_3$, where the phonons contributing appreciably to the SP distortion have energies much higher than the magnetic gap.[41,42] An alternative description of the SP transition, not based on the assumption of phononic adiabaticity, was developed by Uhrig:[41] Phonons are considered as the fast subsystem, responsible for the interchain coupling, and an effective dressed spin model is derived. As a result, the soft phonon is absent and the SP transition is characterized by growing domains of coherent dimerization, whose size diverges at T_{SP}. Alternatively, Gros and Werner[42] showed that no inconsistency is present in the Cross and Fisher theory:[4] They concluded that, in Cross and Fisher framework, a soft phonon has to be present only if the bare phonon frequency satisfies the relation $\Omega_0<2.2\,T_{SP}$. For larger phonon frequencies only a central peak is expected at T_{SP}. However, this new collective excitation, which would consist of the linear superposition of a phonon with two magnons in a singlet state,[42] has not been observed up to now. Moreover, it has been shown that for a detailed understanding of magnetic susceptibility[1,10] and magnetostriction[43,44] data and, at the same time, of the singlet and triplet excitation branches below the continuum,[45,46] the 2D character of the system cannot be neglected.[8,41] In addition, both the NN (J_1) and the NNN (J_2) magnetic exchange interactions have to be taken into account.[44,47,48] $CuGeO_3$ would then be described by an alternating and frustrated AF 1D Heisenberg spin-chain model:

$$H=J\sum_j \{[1+\delta(-1)^i]\mathbf{S}_j\cdot\mathbf{S}_{j+1}+\alpha\mathbf{S}_j\cdot\mathbf{S}_{j+2}\}, \qquad (6)$$

where δ is the static dimerization parameter and $\alpha=J_1/J_2$ is the frustration parameter. In particular, the value $\alpha=0.354$ was obtained,[44,47,48] which is significantly larger than the critical value sufficient for the formation of a spontaneous gap in the magnetic excitation spectrum in absence of lattice dimerization, i.e., $\alpha_c=0.241$.[49,50] However, on the basis of this approach and, in particular, with the large value obtained for α, the amplitude of the dimerization δ, estimated by reproducing the singlet-triplet excitation gap, is substantially underestimated:[51,52] The very small value $\delta\simeq0.012$ is obtained, whereas from the combined analysis of the structural lattice distortion in the dimerized phase and of the magnetoelastic coupling in the uniform phase (from magnetostriction measurements), the value $\delta\simeq0.04-0.05$ results.[53] Still retaining the value $\alpha=0.354$, a consistent value for the lattice dimerization (i.e., of the order of 5%) is obtained from the analysis of the inelastic neutron scattering data if, instead of a static dimerization parameter δ, an explicit coupling between the spins and the three-dimensional phonon system is introduced in the Hamiltonian given in Eq. (6).[54]

Using inelastic neutron scattering and Raman spectroscopy the singlet-triplet magnetic gap was observed,[8,9] sepa-

rated by a second gap from a continuum of magnon excitations,[46,55–57] and a singlet bound state within the two energy gaps.[45,58] Optical spectroscopy is usually not the elective technique to study this kind of process[59] [unless a static (charged magnons[60–62]) or a dynamic (phonon assisted bimagnons[63]) breaking of symmetry is present]. However, a direct singlet-triplet excitation has been observed at 44.3 cm^{-1} in an infrared transmission experiment where the singlet-triplet nature of the transition was demonstrated by the Zeeman splitting of the line in an externally applied magnetic field.[64] This excitation (which has recently been studied also by ESR measurements[65]) is in principle ''doubly'' forbidden: In fact, because of symmetry considerations and of spin conservation we are restricted in an optical experiment to excitations characterized by $k=0$ and $\Delta S=0$. In Ref. 25 we showed that this transition exists for polarized light with $E\perp$ chain (Fig. 5, top) and is absent with $E\|$ chain (Fig. 5, bottom), in contradiction to the polarization dependence calculated by Uhrig[66] for the mechanism where the excitation across the gap at the wave vector $(0,2\pi/b,0)$ in the Brillouin zone is activated by the existence of staggered magnetic fields along the direction perpendicular to the chains. A second singlet-triplet (optical) branch with a gap value at the Γ point of ~ 5.8 meV was observed by Lorenzo *et al.*[67] in neutron scattering measurements. The dispersion of this newly found optical mode is identical to the one of the acoustic mode, but shifted by $(2\pi/b+\pi/c)$. Lorenzo *et al.*[67] proposed that the origin of this second mode is the relative orientation of the Cu-O(2)-Cu units between next-neighboring chains along the *b* axis, along with a small spin-orbit coupling. This would give rise the slight distortion of the spin isotropy necessary to reproduce the finite intensity for the optical triplet mode and the difference in the scattering intensities between the optical and the acoustic branches.[67] On the other hand, anisotropy in the magnetic exchange constants along the *b* axis below T_{SP} ought to be present in the space group $P2_12_12_1$ proposed by Yamada *et al.*[30,31] This property is due to the strong fluctuations of the exchange interactions expected upon decreasing the temperature toward T_{SP}. These results not only show that the structure generally assumed for $CuGeO_3$ in the uniform phase may be incorrect, but they also suggest a possible explanation for the singlet-triplet excitation in the optical spectra at $\sim 44-5.5$ meV: Such an optical transition, with approximately the right energy value, is now present at $k=0$ and not only at $\mathbf{k}=(0,2\pi/b,0)$, which is inaccessible in an optical experiment. In this context, the reason why the final constraint $\Delta S=0$ is not satisfied might be spin-orbit interaction, which could be strong enough to relax the spin conservation rule. In order to assess whether this absorption line is due to an electric dipole or to a magnetic dipole transition, in presence of spin-orbit interaction, a careful analysis of selection rules and absolute intensities is needed.

VII. CONCLUSIONS

We reported the temperature-dependent optical response of pure and doped $CuGeO_3$ in the frequency range 20–32 000 cm^{-1} with particular emphasis on the infrared phonon spectra. We detected zone-boundary folded modes activated by the SP phase transition. Following the temperature dependence of these modes we were able to determine the second-order character of the phase transition and to study the effect of doping on T_{SP}: In particular, we showed that the substitution of Ge with Si is three times more efficient, than the one of Cu with Mg, in reducing T_{SP}. This was explained, following Khomskii and co-workers,[36,37] as a consequence of the side-group effect. We discussed the optical activity of the direct singlet-triplet excitation across the magnetic gap in relation to newly reported inelastic neutron scattering data that show the existence of a second (optical) magnetic branch.[67] The anisotropy in the magnetic exchange constants along the *b* axis, necessary for the optical triplet mode in order to gain a finite intensity and, possibly, the strong changes in the phonon spectra of Si-substituted samples can be understood in terms of the alternative space group $P2_12_12_1$, recently proposed for $CuGeO_3$ in the high-temperature phase.[30,31]

ACKNOWLEDGMENTS

We gratefully acknowledge M. Mostovoy and D.I. Khomskii for stimulating discussions and P.H.M. van Loosdrecht, J.E. Lorenzo, and M. Grüninger for many useful comments. Andrea Damascelli is pleased to thank M. Picchietto and B. Topí for assistance. This investigation was supported by the Netherlands Foundation for Fundamental Research on Matter (FOM) with financial aid from the Nederlandse Organisatie voor Wetenschappelijk Onderzoek (NWO).

*Present address: Laboratory for Advanced Materials, McCullough Building, Stanford University, 476 Lomita Mall, Stanford, CA 94305-4045. Electronic address: damascel@stanford.edu

[1] M. Hase, I. Terasaki, and K. Uchinokura, Phys. Rev. Lett. **70**, 3651 (1993).
[2] H. Völlenkle, A. Wittmann, and H. Nowotny, Monatsch. Chem. **98**, 1352 (1967).
[3] E. Pytte, Phys. Rev. B **10**, 4637 (1974).
[4] M.C. Cross, and D.S. Fisher, Phys. Rev. B **19**, 402 (1979).
[5] L.N. Bulaevskii, A.I. Buzdin, and D.I. Khomskii, Solid State Commun. **27**, 5 (1978).
[6] M.C. Cross, Phys. Rev. B **20**, 4606 (1979).
[7] For a review, see J.P. Boucher, and L.P. Regnault, J. Phys. I **6**, 1939 (1996).
[8] M. Nishi, O. Fujita, and J. Akimitsu, Phys. Rev. B **50**, 6508 (1994).
[9] O. Fujita, J. Akimitsu, M. Nishi, and K. Kakurai, Phys. Rev. Lett. **74**, 1677 (1995).
[10] J.P. Pouget, L.P. Regnault, M. Aïn, B. Hennion, J.-P. Renard, P. Veillet, G. Dhalenne, and A. Revcolevschi, Phys. Rev. Lett. **72**, 4037 (1994).
[11] K. Hirota, D.E. Cox, J.E. Lorenzo, G. Shirane, J.M. Tranquada, M. Hase, K. Uchinokura, H. Kojima, Y. Shibuya, and I. Tanaka, Phys. Rev. Lett. **73**, 736 (1994).
[12] M. Braden, G. Wilkendorf, J. Lorenzana, M. Aïn, G.J. McIntyre, M. Behruzi, G. Heger, G. Dhalenne, and A. Revcolevschi, Phys. Rev. B **54**, 1105 (1996).
[13] M. Hase, I. Terasaki, K. Uchinokura, M. Tokunaga, N. Miura, and H. Obara, Phys. Rev. B **48**, 9616 (1993).
[14] T. Lorenz, U. Ammerahl, T. Auweiler, B. Büchner, A. Rev-

colevschi, and G. Dhalenne, Phys. Rev. B **55**, 5914 (1997).
[15] J.W. Bray, H.R. Hart, L.V. Interrante, I.S. Jacobs, J.S. Kasper, G.D. Watkins, and S.H. Wee, Phys. Rev. Lett. **35**, 744 (1975).
[16] I.S. Jacobs, J.W. Bray, H.R. Hart, L.V. Interrante, J.S. Kasper, G.D. Watkins, D.E. Prober, and J.C. Bonner, Phys. Rev. B **14**, 3036 (1976).
[17] S. Huizinga, J. Kommandeur, G.A. Sawatzky, B.T. Thole, K. Kopinga, W.J.M. de Jonge, and J. Roos, Phys. Rev. B **19**, 4723 (1979).
[18] A. Damascelli, D. van der Marel, F. Parmigiani, G. Dhalenne, and A. Revcolevschi, Physica B **244**, 114 (1998).
[19] D.L. Rousseau, R.P. Bauman, and S.P.S. Porto, J. Raman Spectrosc. **10**, 253 (1981).
[20] Z.V. Popović, S.D. Dević, V.N. Popov, G. Dhalenne, and A. Revcolevschi, Phys. Rev. B **52**, 4185 (1995).
[21] A. Revcolevschi and G. Dhalenne, Adv. Mater. **5**, 657 (1993).
[22] M.V. Klein and T.E. Furtak, *Optics* (Wiley, New York, 1983).
[23] I. Terasaki, R. Itti, N. Koshizuka, M. Hase, I. Tsukada, and K. Uchinokur, Phys. Rev. B **52**, 295 (1995).
[24] M. Bassi, P. Camagni, R. Rolli, G. Samoggia, F. Parmigiani, G. Dhalenne, and A. Revcolevschi, Phys. Rev. B **54**, R11 030 (1996).
[25] A. Damascelli, D. van der Marel, F. Parmigiani, G. Dhalenne, and A. Revcolevschi, Phys. Rev. B **56**, R11 373 (1997).
[26] M.N. Popova, A.B. Sushkov, S.A. Golubchik, A.N. Vasil'ev, and L.I. Leonyuk, Phys. Rev. B **57**, 5040 (1998).
[27] For a detailed description of the backward wave oscillator and its use in (sub)millimeter spectroscopy on solids, see G. Kozlov and A. Volkov, *Millimeter Wave Spectroscopy on Solids* edited by G. Grüner (Springer Verlag, New York, 1995).
[28] M. Braden, B. Hennion, W. Reichardt, G. Dhalenne, and A. Revcolevschi, Phys. Rev. Lett. **80**, 3634 (1998).
[29] A.D. Bruce and R.A. Cowley, *Structural Phase Transitions* (Taylor & Francis, London, 1981).
[30] I. Yamada, M. Nishi, and J. Akimitsu, J. Phys.: Condens. Matter **8**, 2625 (1996).
[31] M. Hidaka, M. Hatae, I. Yamada, M. Nishi, and J. Akimitsu, J. Phys.: Condens. Matter **9**, 809 (1997).
[32] M.D. Lumsden, B.D. Gaulin, H. Dabkowska, and M.L. Plumer, Phys. Rev. Lett. **76**, 4919 (1996).
[33] D.E. Moncton, R.J. Birgeneau, L.V. Interrante, and F. Wudl, Phys. Rev. Lett. **39**, 507 (1977).
[34] L.P. Regnault, J.-P. Renard, G. Dhalenne, and A. Revcolevschi, Europhys. Lett. **32**, 579 (1995).
[35] B. Grenier, J.-P. Renard, P. Veillet, C. Paulsen, G. Dhalenne, and A. Revcolevschi, Phys. Rev. B **58**, 8202 (1998).
[36] W. Geertsma and D. Khomskii, Phys. Rev. B **54**, 3011 (1996).
[37] D. Khomskii, W. Geertsma, and M. Mostovoy, Czech. J. Phys. **46**, 3239 (1996).
[38] J. Goodenough, *Magnetism and the Chemical Bond* (Wiley, New York, 1963).
[39] For a review, see M.A. Kastner, R.J. Birgeneau, G. Shirane, and Y. Endoh, Rev. Mod. Phys. **70**, 897 (1998), and references therein.
[40] M. Grüninger, D. van der Marel, A. Damascelli, A. Zibold, H.P. Geserich, A. Erb, M. Kläser, Th. Wolf, T. Nunner, and T. Kopp, Physica C **317-318**, 286 (1999).
[41] G.S. Uhrig, Phys. Rev. B **57**, R14 004 (1998).
[42] C. Gros and R. Werner, Phys. Rev. B **58**, R14 677 (1998).
[43] B. Büchner, U. Ammerahl, T. Lorenz, W. Brenig, G. Dhalenne, and A. Revcolevschi, Phys. Rev. Lett. **77**, 1624 (1996).
[44] T. Lorenz, B. Büchner, P.H.M. van Loosdrecht, F. Schönfeld, G. Chouteau, A. Revcolevschi, and G. Dhalenne, Phys. Rev. Lett. **81**, 148 (1998).
[45] G. Els, P.H.M. van Loosdrecht, P. Lemmens, H. Vonberg, G. Güntherodt, G.S. Uhrig, O. Fujita, J. Akimitsu, G. Dhalenne, and A. Revcolevschi, Phys. Rev. Lett. **79**, 5138 (1997).
[46] M. Aïn, J.E. Lorenzo, L.P. Regnault, G. Dhalenne, A. Revcolevschi, B. Hennion, and Th. Jolicoeur, Phys. Rev. Lett. **78**, 1560 (1997).
[47] K. Fabricius, A. Klümper, U. Löw, B. Büchner, T. Lorenz, G. Dhalenne, and A. Revcolevschi, Phys. Rev. B **57**, 1102 (1998).
[48] G. Bouzerar, A.P. Kampf, and G.I. Japaridze, Phys. Rev. B **58**, 3117 (1998).
[49] G. Castilla, S. Chakravarty, and V.J. Emery, Phys. Rev. Lett. **75**, 1823 (1995).
[50] K. Okamoto and K. Nomura, Phys. Lett. A **169**, 433 (1993).
[51] J. Riera and A. Dobry, Phys. Rev. B **51**, 16 098 (1995).
[52] G. Bouzerar, A.P. Kampf, and F. Schönfeld, cond-mat/9701176 (unpublished).
[53] B. Büchner, H. Fehske, A.P. Kampf, and G. Wellein, Physica B **259-261**, 956 (1999).
[54] G. Wellein, H. Fehske, and A.P. Kampf, Phys. Rev. Lett. **81**, 3956 (1998).
[55] M. Arai, M. Fujita, M. Motokawa, J. Akimitsu, and S.M. Bennington, Phys. Rev. Lett. **77**, 3649 (1996).
[56] H. Kuroe, T. Sekine, M. Hase, Y. Sasago, K. Uchinokura, H. Kojima, I. Tanaka, and Y. Shibuya, Phys. Rev. B **50**, R16 468 (1994).
[57] P.H.M. van Loosdrecht, J.P. Boucher, G. Martinez, G. Dhalenne, and A. Revcolevschi, Phys. Rev. Lett. **76**, 311 (1996).
[58] P.H.M. van Loosdrecht, J. Zeman, G. Martinez, G. Dhalenne, and A. Revcolevschi, Phys. Rev. Lett. **78**, 487 (1997).
[59] A. Damascelli, Ph.D. thesis, Groningen University, 1999. The complete thesis in PDF files is available at this URL: http://www.ub.rug.nl/eldoc/dis/science/a.damascelli/
[60] A. Damascelli, D. van der Marel, M. Grüninger, C. Presura, T.T.M. Palstra, J. Jegoudez, and A. Revcolevschi, Phys. Rev. Lett. **81**, 918 (1998).
[61] A. Damascelli, D. van der Marel, J. Jegoudez, G. Dhalenne, and A. Revcolevschi, Physica B **259-261**, 978 (1999).
[62] A. Damascelli, C. Presura, D. van der Marel, J. Jegoudez, and A. Revcolevschi, Phys. Rev. B **61**, 2535 (2000).
[63] J. Lorenzana and G.A. Sawatzky, Phys. Rev. Lett. **74**, 1867 (1995).
[64] P.H.M. van Loosdrecht, S. Huant, G. Martinez, G. Dhalenne, and A. Revcolevschi, Phys. Rev. B **54**, R3730 (1996).
[65] H. Nojiri, H. Ohta, S. Okubo, O. Fujita, J. Akimitsu, and M. Motokawa, J. Phys. Soc. Jpn. **68**, 3417 (1999).
[66] G.S. Uhrig, Phys. Rev. Lett. **79**, 163 (1997).
[67] J.E. Lorenzo, L.P. Regnault, J.P. Boucher, B. Hennion, G. Dhalenne, and A. Revcolevschi, Europhys. Lett. **45**, 619 (1999).